(12)

SRI International

AD-A257 385

Annual Report • October 1992

EVALUATION OF A DIFFUSION/TRAPPING MODEL FOR HYDROGEN INGRESS IN HIGH-STRENGTH ALLOYS

Bruce G. Pound, Group Leader
Corrosion Science and Technology
Materials Research Center

SRI Project PYU-2969

DTIC
S ELECTE
NOV1 2 1992
C D

Prepared for:

Department of the Navy
Office of Naval Research
800 N. Quincy Street
Arlington, VA 22217

Attn: Dr. A. J. Sedriks

DISTRIBUTION STATEMENT A

Approved for public release;
Distribution Unlimited

Contract No. N00014-91-C-0263

Approved:

R. Thomas Podoll
Laboratory Director
Materials and Chemical Engineering Laboratory

David M. Golden
Vice President
Physical Sciences Division

92-29335

REPORT DOCUMENTATION PAGE

Public reporting burden for this collection of information is estimated to average 1 hour per response, including the time for reviewing instructions, searching existing data sources, gathering and maintaining the data needed, and completing and reviewing the collection of information. Send comments regarding this burden estimate or any other aspect of this collection of information, including suggestions for reducing this burden, to Washington Headquarters Services, Directorate for Information Operations and Reports, 1215 Jefferson Davis Highway, Suite 1204, Arlington, VA 22202-4302, and to the Office of Management and Budget, Paperwork Reduction Project (0704-0188), Washington, DC 20503.

1. AGENCY USE ONLY (Leave blank)	2. REPORT DATE Oct 92	3. REPORT TYPE AND DATES COVERED Annual 15 Sept 91-15 Sept 92

4. TITLE AND SUBTITLE	5. FUNDING NUMBERS
Evaluation of a Diffusion/Trapping Model for Hydrogen Ingress in High-Strength Alloys.	N00014-91-C-0263

6. AUTHOR(S)

Bruce G. Pound

7. PERFORMING ORGANIZATION NAME(S) AND ADDRESS(ES)	8. PERFORMING ORGANIZATION REPORT NUMBER
SRI International 333 Ravenswood Ave. Menlo Park, CA 94025	PYU-2969

9. SPONSORING/MONITORING AGENCY NAME(S) AND ADDRESS(ES)	10. SPONSORING/MONITORING AGENCY REPORT NUMBER
Office of Naval Research 800 N. Quincy St. Arlington, VA 22217-5000	

11. SUPPLEMENTARY NOTES

12a. DISTRIBUTION/AVAILABILITY STATEMENT	12b. DISTRIBUTION CODE
Approved for public release - distribution unlimited	

13. ABSTRACT (Maximum 200 words)

Alloys developed to improve properties such as strength, weight, and corrosion resistance often show decreased resistance to hydrogen embrittlement. The objective of this research was to determine the hydrogen ingress behavior of high performance alloys, particularly in terms of irreversible trapping, with a view to characterizing their interaction with hydrogen and resulting susceptibility to hydrogen embrittlement. A technique referred to as hydrogen ingress analysis by potentiostatic pulsing (HIAPP) was applied to three beta-titanium alloys (Beta-C, Ti-10V-2Fe-3Al, and Ti-13V-11Cr-3Al), an alpha-beta titanium alloy (Ti-6Al-4V), and two copper-nickel alloys (Marinel and Monel K-500). Anodic current transients were obtained for these alloys in an acetate buffer (1 mol/L HAc-1 mol/L NaAc where Ac = acetate) and analyzed using a diffusion/trapping model under interface control conditions to evaluate the trapping constant and hydrogen entry flux. A marked increase observed in the trapping constants for the beta-titanium alloys with aging is attributed to precipitation of the secondary alpha phase. Aging also affects the passive film and therefore the hydrogen entry flux. The trapping constants for aged Marinel and Monel K-500 are not considered to differ significantly, but a smaller entry flux for the Marinel appears to account, at least partly, for the lower susceptibility to hydrogen embrittlement reported for Marinel.

14. SUBJECT TERMS			15. NUMBER OF PAGES 35
Beta-Titanium Alloys, Monel K-500, Marinel, Potentiostatic Pulse Hydrogen Trapping, Trapping Model, Hydrogen Ingress			16. PRICE CODE

17. SECURITY CLASSIFICATION OF REPORT	18. SECURITY CLASSIFICATION OF THIS PAGE	19. SECURITY CLASSIFICATION OF ABSTRACT	20. LIMITATION OF ABSTRACT
UNCLASSIFIED	UNCLASSIFIED	UNCLASSIFIED	UL

ACKNOWLEDGEMENTS

DTIC QUALITY INSPECTED 4

Accession For	
NTIS GRA&I	☑
DTIC TAB	☐
Unannounced	☐
Justification	
By	
Distribution/	
Availability Codes	
Dist	Avail and/or Special
A-1	

ii

CONTENTS

ILLUSTRATIONS

TABLES

INTRODUCTION

High-performance alloys are increasingly being required to meet improved levels of strength, weight, and corrosion resistance in naval applications. In particular, β-titanium alloys, which can be aged to yield strengths in the region of 1200 MPa (170 ksi) or higher, are attractive as lightweight materials for airframe components subject to high stresses. Most hydrogen embrittlement studies of titanium alloys have focused on the α–β type, and relatively little work has been performed on β alloys. Nevertheless, β-Ti alloys have been found to undergo a loss in ductility, despite having a high solubility of hydrogen.[1,2] Clearly, the propensity of these alloys to hydrogen embrittlement needs to be better understood.

The susceptibility of alloys to hydrogen embrittlement is strongly affected by the interaction of hydrogen with microstructural heterogeneities that act as hydrogen traps. In particular, traps with a large saturability and a high binding energy for hydrogen are regarded as highly conducive to hydrogen embrittlement. Consequently, characterization of high-strength alloys in terms of these irreversible traps can assist in determining their susceptibility to embrittlement.

In this program, the entry and trapping of hydrogen in various high-strength alloys has been investigated by using a technique referred to as hydrogen ingress analysis by potentiostatic pulsing (HIAPP).[3-7] As the name indicates, the alloy of interest is subjected to a potentiostatic pulse and the resulting current transients are analyzed by using a model for hydrogen diffusion and trapping.[8,9] During previous work, HIAPP was applied to a high-strength steel,[3,4] precipitation-hardened and work-hardened nickel-base alloys,[3-6] and titanium[7] and was shown to be effective in evaluating the trapping characteristics of alloys containing both single and multiple principal traps. The results showed that a range of microstructural features can be identified as the principal irreversible traps and thus demonstrated the ability of HIAPP to provide a basis for explaining differences in the resistance of alloys to hydrogen embrittlement. Perhaps more important, it was established that the trapping capability of the alloys can be correlated with the variation in known susceptibility to hydrogen embrittlement; that is, HIAPP provides a means of predicting the embrittlement susceptibility of alloys.

1

During the present phase of the program, the use of HIAPP was extended to ß-titanium alloys—Beta-C, Ti-10V-2Fe-3Al (commonly referred to as Ti-10-2-3), and Ti-13V-11Cr-3Al (Ti-13-11-3); an α-β titanium alloy—Ti-6Al-4V (Ti-6-4); and Marinel, a recently developed copper-nickel alloy. The objective was to determine the hydrogen ingress behavior (particularly in terms of trapping) of the individual alloys, with a view to characterizing both their interaction with hydrogen and their susceptibility to hydrogen embrittlement.

EXPERIMENTAL PROCEDURE

MATERIALS

Titanium Alloys

The composition of each alloy was provided by the producer and is given in Table 1. The Ti-10-2-3 alloy was supplied by Timet Corporation as an α-β finish-rolled plate (25 mm thick) that was subsequently solution treated at 820°C for 1 h, water quenched, and aged at 560°C for 1 h in a salt bath. The β-solution (820°C) treatment produced a microstructure that was devoid of primary α phase. However, aging resulted in the precipitation of a fine secondary α phase within the grains and at the grain boundaries. The grain size varied between approximately 50 and 300 μm. The aged material had a yield strength of 1372 MPa (199 ksi). A rod 1.27 cm in diameter was machined from the heat treated plate for use as an electrode.

The Beta-C alloy was supplied by RMI Titanium Company as rod that had been hot-rolled, annealed, and centerless ground. The diameter of the rod was 1.593 cm. The yield strength of the as-received (unaged) alloy was given as 864-878 MPa (125-127 ksi). A section of rod was aged at 510°C for 20 h and air cooled to produce a yield strength of 1208-1223 MPa (175-177 ksi). The alloy was used in both the unaged and aged condition to determine the effect of the secondary α phase on hydrogen trapping.

The Ti-13-11-3 alloy was supplied by Astro Metallurgical as cold drawn rod with a diameter of 0.953 cm. Although the alloy is usually solution treated at various stages during drawing, primary α phase can be present as a result of cold work.[10] The yield strength of the as-received (unaged) alloy was unavailable. A section of rod was aged at 427°C for 10 h and air cooled to produce a yield strength of 1310-1379 MPa (190-200 ksi). This alloy was also tested in both the unaged and aged condition.

The α-β alloy (Ti-6-4) was produced by Timet as rod with a diameter of 1.27 cm and was used as-received; its yield strength was 1027 MPa (149 ksi).

Table 1
COMPOSITION OF TITANIUM ALLOYS*

Element	TI-10-2-3	TI-13-11-3	Beta-C	TI-6-4
Al	3.025	3.14	3.0	6.40
B	0.001			0.001
C	0.017	0.010	0.01	0.016
Cr		11.41	6.0	
Cu	0.001			0.002
Fe	1.945	0.12	0.06	0.16
Mn	0.004			0.006
Mo	0.031		3.9	0.006
N	0.008	0.013	0.018	0.009
O	0.097	0.097	0.093	0.19
Si	0.039			0.012
Sn	0.010			
Ti	Bal.	Bal.	Bal.	Bal.
V	9.795	13.82	8.0	4.10
Zr	0.001		3.8	
H	1 ppm	0.0178	97 ppm	0.007
Other		Y < 0.005	Nb 0.10 Y <50 ppm	

* wt% unless indicated.

Copper-Nickel Alloys

The composition of the Marinel was provided by the producer and is given in Table 2. Also shown is the composition of Monel K-500, a 65 Ni-30 Cu alloy that was examined in Phase I of our study[3,4] and is included here because its hydrogen characteristics provided a useful comparison with those of the 77 Cu-15 Ni-containing Marinel. Although the Monel had been examined previously, subsequent refinements to both the pulse technique and the analysis made it worthwhile to redetermine its hydrogen ingress parameters in the present tests.

The Marinel was provided by Langley Alloys as rod with a diameter of 2.4 cm. The as-received alloy had been aged to a yield strength of 793 MPa (115 ksi) and was not treated further.

The Monel K-500 had been supplied previously by Huntington Alloys as an unaged, 1.27-cm-diameter, cold-drawn rod with a yield strength of about 758 MPa (110 ksi). A section of the rod was age-hardened to give a yield strength of about 1096 MPa (159 ksi).

Table 2
COMPOSITION (wt%) OF COPPER-NICKEL ALLOYS

Element	Marinel	Monel K-500
Al	1.61	2.92
C	0.010	0.16
Cr	0.40	-
Cu	76.8	29.99
Fe	0.96	0.64
Mg	0.02	-
Mn	4.36	0.72
Ni	15.00	64.96
P	0.010	-
Pb	0.007	-
S	0.005	0.001
Si	0.05	0.15
Sn	<0.02	-
Ti	-	0.46
Zn	0.02	-
Zr	0.69	-

TECHNIQUE

Details of the electrochemical cell and instrumentation have been given previously.[2] The test electrodes of each alloy consisted of a length (1.3-3.8 cm) of rod press-fitted into a Teflon sheath so that only the planar end surface was exposed to the electrolyte. The surface was polished before each experiment with SiC paper followed by 0.05-μm alumina powder. The electrolyte was an acetate buffer (1 mol L^{-1} acetic acid/1 mol L^{-1} sodium acetate) containing 15 ppm As$_2$O$_3$ as a hydrogen entry promoter. The electrolyte was deaerated with argon for 1 h before measurements began and throughout data acquisition. The potentials were measured with respect to a saturated calomel electrode (SCE). All tests were performed at 22 $\pm$ 1°C.

The test electrode was charged with hydrogen at a constant potential E$_c$ for a time t$_c$, after which the potential was stepped to a more positive value E$_A$ (10 mV negative of the open-circuit potential E$_{oc}$).[2,7,8] The charging time was varied from 5 s to 60 s. Anodic current transients with a charge q$_a$ were obtained for each charging time over a range of overpotentials (η = E$_c$ - E$_{oc}$). The open-circuit potential of the test electrode was sampled immediately before each charging time and was also used to monitor the stability of the surface oxide.

ANALYSIS

DIFFUSION/TRAPPING MODEL

The anodic current transients were analyzed using a diffusion/trapping model[8] based on interface-modified diffusion control (often referred to simply as interface control). Under these conditions, the rate of hydrogen ingress in an alloy is controlled by diffusion but the entry flux of hydrogen across the interface is restricted; in the case of pure diffusion control, hydrogen entry is assumed to be fast enough that equilibrium is rapidly achieved between adsorbed and subsurface hydrogen. According to the interface control model, the total charge passed out is given in nondimensional form by

$$Q'(\infty) = R^{1/2}\{1 - e^{-R}/(\pi R)^{1/2} - [1 - 1/(2R)]\text{erf}(R^{1/2})\} \tag{1}$$

The nondimensional terms are defined by $Q = q/[FJ\sqrt{(t_c/k_a)^{1/2}}]$ and $R = k_a t_c$, where q is the dimensionalized charge in C cm^{-2}, F is the Faraday constant, and J is the ingress flux in mol cm^{-2} s^{-1}. The charge $q'(\infty)$ corresponding to $Q'(\infty)$ is equated to q_a; the adsorbed charge is invariably found to be negligible, and so q_a can be associated entirely with absorbed hydrogen. k_a is an apparent trapping constant measured for irreversible traps in the presence of reversible traps and can be expressed by $k(D_a/D_L)$ where k is the irreversible trapping constant, D_a is the apparent diffusivity, and D_L is the lattice diffusivity of hydrogen in the metal.

In all cases, Eq. (1) could be fitted to data for q_a to obtain values of k_a and J such that J was constant over the range of charging times and k_a was essentially independent of charging potential, as is required for the model to be valid. The values of k_a and J can be used to calculate the irreversibly trapped charge (q_T) given nondimensionally by

$$Q_T = [R^{1/2} - 1/(2R^{1/2})]\text{erf}(R^{1/2}) + e^{-R}/\pi^{1/2} \tag{2}$$

The charge associated with the entry of hydrogen into the metal (q_{in}) can be determined from its nondimensional form of $Q_{in} = R^{1/2}$, and so the fraction of the hydrogen, q_T/q_{in}, in the metal that is trapped can be found.

The density of particles providing irreversible traps (N_i) can be obtained from the apparent trapping constant by using a model based on spherical traps:[5]

$$N_i = k_a a / (4\pi d^2 D_a) \tag{3}$$

where a is the diameter of the metal atom and d is the trap radius, which is estimated from the dimensions of heterogeneities that are potential irreversible traps. The dominant irreversible trap can be identified by comparing the calculated trap density with the actual concentration of a particular heterogeneity in the alloy.

The assumption of spherical traps in the above model is an approximation in most cases, but for alloys studied previously, the concentrations of potential trap particles that are clearly not spherical have shown close agreement with the calculated trap density, suggesting that the incorporation of a more applicable trap geometry will make little difference in identifying the principal traps.

TITANIUM ALLOYS

Ti-10V-2Fe-3Al

Values of k_a and J for six tests are shown in Table 3. Although k_a was essentially independent of charging potential, it did show some variation between tests. This variation is attributed to differences in the amount of α phase at grain boundaries accessible to hydrogen, the differences resulting from the variation in grain size (50-300 μm). The mean value of k_a for all the tests is 0.066 ± 0.009 s^{-1}. As would be expected for the diffusion/trapping model, the flux increases with potential because of its dependence on the surface coverage of adsorbed hydrogen.

Beta-C Ti

The open-circuit potentials for the aged alloy were typically 200-300 mV more negative than those for the unaged alloy. Hence, the charging potential (E_c) for the aged alloy was correspondingly more negative at a given overpotential. Nevertheless, the values of q_a at the same overpotential were typically a factor of 2 to 4 times smaller than those for the unaged alloy. The smaller values of q_a for the aged alloy, as discussed below, resulted

from both a decrease in the amount of hydrogen absorbed and an increase in the proportion of the absorbed hydrogen being trapped. Thus, aging produces two opposing effects in terms of hydrogen embrittlement: the apparent change in the passive film (as reflected by E_{oc}) reduces hydrogen entry, whereas precipitation of the α phase appears to be the likely cause of the enhanced trapping capability.

Table 3
VALUES OF k_a AND J FOR TI-10V-2Fe-3AI

Test	η (V)	E_c (V/SCE)	k_a (s^{-1})	J (nmol cm^{-2} s^{-1})	Mean k_a
1	-0.45	-0.546	0.073	0.175	
	-0.50	-0.589	0.073	0.192	0.072 ± 0.001
	-0.55	-0.650	0.070	0.191	
2	-0.50	-0.609	0.043	0.133	
	-0.55	-0.666	0.049	0.161	0.048 ± 0.003
	-0.60	-0.726	0.052	0.198	
3	-0.45	-0.729	0.059	0.151	
	-0.50	-0.792	0.066	0.230	0.063 ± 0.003
4	-0.50	-0.740	0.065	0.377	
	-0.55	-0.814	0.068	0.481	0.067 ± 0.002
5	-0.45	-0.780	0.074	0.285	
	-0.50	-0.851	0.075	0.422	0.075 ± 0.001
6	-0.45	-0.764	0.080	0.295	
	-0.50	-0.839	0.081	0.428	0.081 ± 0.001

The variation in q_a with charging time was considerably less pronounced for the aged alloy; this effect is also due to the smaller amount of absorbed hydrogen and particularly to the increase in trapping capability, as shown below. The smaller variation in q_a for the aged alloy is probably responsible for the greater scatter usually observed in the trapping constants for the aged β-Ti alloys in a particular test. Values of k_a and J for two tests on both the unaged and aged Beta-C alloy are given in Table 4. In both cases, k_a was independent of charging potential, although some scatter, as noted above, occurred with the aged alloy. The overall mean values of k_a for the unaged and aged alloys were 0.031 ±

9

0.002 s^{-1} and 0.088 ± 0.010 s^{-1}, respectively. As with Ti-10-2-3, the entry flux showed the expected increase with potential for both conditions of the alloy, but it was decreased by aging.

Table 4
VALUES OF k_a AND J FOR BETA-C TI

State	Test	η (V)	E_c (V/SCE)	k_a (s^{-1})	J (nmol cm^{-2} s^{-1})	Mean k_a
Unaged	7	-0.35	-0.455	0.036	0.095	
		-0.40	-0.503	0.032	0.103	
		-0.45	-0.553	0.028	0.109	0.032 ± 0.002
		-0.50	-0.607	0.032	0.133	
		-0.55	-0.660	0.033	0.159	
	8	-0.35	-0.479	0.030	0.083	
		-0.40	-0.521	0.029	0.100	
		-0.45	-0.570	0.031	0.121	0.030 ± 0.001
		-0.50	-0.620	0.032	0.146	
		-0.55	-0.672	0.030	0.169	
Aged	9	-0.40	-0.800	0.086	0.047	
		-0.45	-0.834	0.074	0.057	0.083 ± 0.011
		-0.55	-0.911	0.070	0.092	
		-0.60	-0.967	0.101	0.159	
	10	-0.45	-0.781	0.095	0.082	
		-0.50	-0.826	0.097	0.107	0.092 ± 0.006
		-0.55	-0.859	0.081	0.115	
		-0.60	-0.926	0.096	0.212	

Values of q_{in}, q_T, and q_T/q_{in} calculated using the results for k_a and J at η = -0.45 V are shown in Figs. 1 (q_{in} and q_T) and 2 (q_T/q_{in}). As to be expected, the decrease in J produced by aging causes a marked decrease in q_{in}, but the corresponding decrease in q_T is lessened because of the higher k_a for the aged alloy. The effect of k_a alone without J can be examined by considering the ratio of q_T to q_{in}, and it is clear from Fig. 2 that the proportion of hydrogen trapped is greater for the aged alloy. The data for q_T/q_{in} are of course independent of potential, since each component has the same dependence on flux.
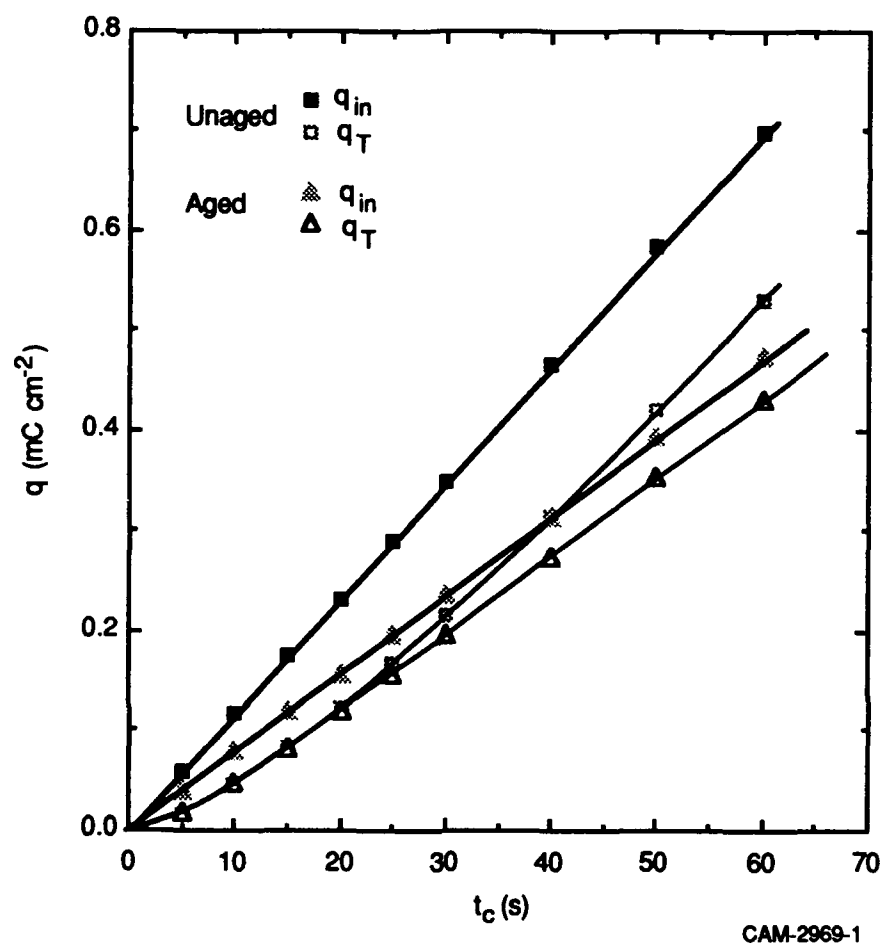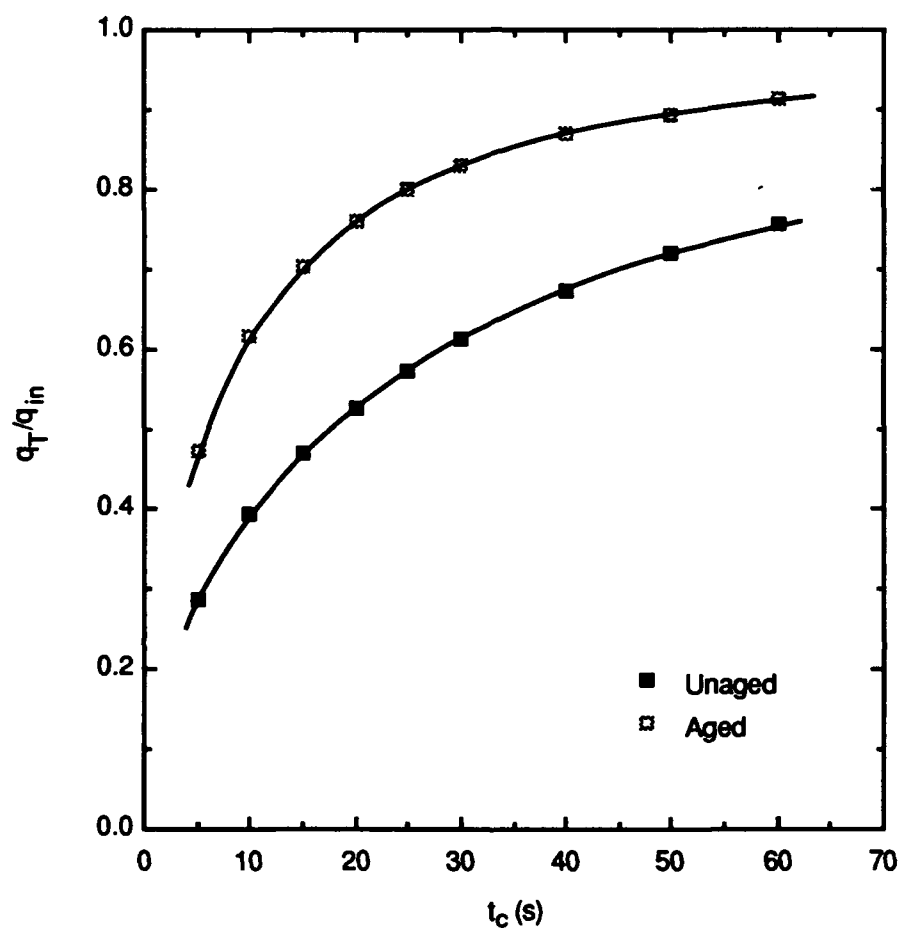
10

Figure 1. Dependence of q_{in} and q_T on charging time for Beta-C Ti.
$\eta = -0.45$ V.

CAM-2969-1

11

CAM-2969-2

Figure 2. Dependence of q_T/q_{in} on charging time for Beta-C Ti.
$\eta = -0.45$ V.

The anodic charge (q_a) is simply the difference between q_{in} and q_T, and so, as noted above, the changes in q_a with aging can readily be attributed to the changes in J and k_a. The difference, $q_{in} - q_T$, can be expanded to yield

$$q_a = FJ[t_c - (t_c/k_a)^{1/2}Q_T] \qquad (4)$$

where Q_T is a multiterm function of k_a and t_c [Eq. (2)], and so it is not obvious whether the decrease observed in q_a for Beta-C Ti is caused primarily by the decrease in J or the increase in k_a. However, the individual effects of J and k_a can be examined by calculating q_a from Eq. (4) for different cases. The variation in q_a with t_c for $\eta = -0.45$ V is shown in Fig. 3. Calculated values for the unaged and aged alloys are represented by the top and bottom curves (1 and 4), respectively, whereas the two middle curves (2 and 3) are hybrids of these cases. It is apparent that the decrease in q_a is somewhat greater with an increase in k_a (curve 3) than with a decrease in J (curve 2). Moreover, the higher k_a appears to be primarily responsible for restricting the increase in q_a with t_c; that is, the curve tends to flatten as k_a becomes larger.

Ti-13V-11Cr-3Al

The open-circuit potentials for the aged alloy were typically 400-500 mV more negative than those for the unaged alloy. In addition, the values of q_a were relatively small (<0.05 mC cm^{-2}) for unaged Ti-13-11-3, and — unlike the situation with Beta-C Ti — they were smaller than those for the aged alloy at higher overpotentials (-0.50 to -0.60 V). Nevertheless, even at $\eta = -0.60$ V, the unaged and aged alloys differed in q_a by a factor of less than 3.

The unaged (cold drawn) Ti-13-11-3 presumably contained primary α phase, so on the basis of the results for aged Beta-C Ti, the small values in q_a are probably indicative of restricted hydrogen entry coupled with considerable trapping. The increase in q_a with aging suggests that the amount of hydrogen entering the aged alloy exceeds that lost to additional trapping introduced by the secondary α phase. In the case of aged alloy, the change in q_a with charging time was very small and poorly defined within the precision of the data, so only rough values could be estimated for k_a and J. The unaged alloy showed a slightly greater increase in q_a, such that more reliable values of k_a and J could be obtained in this case.
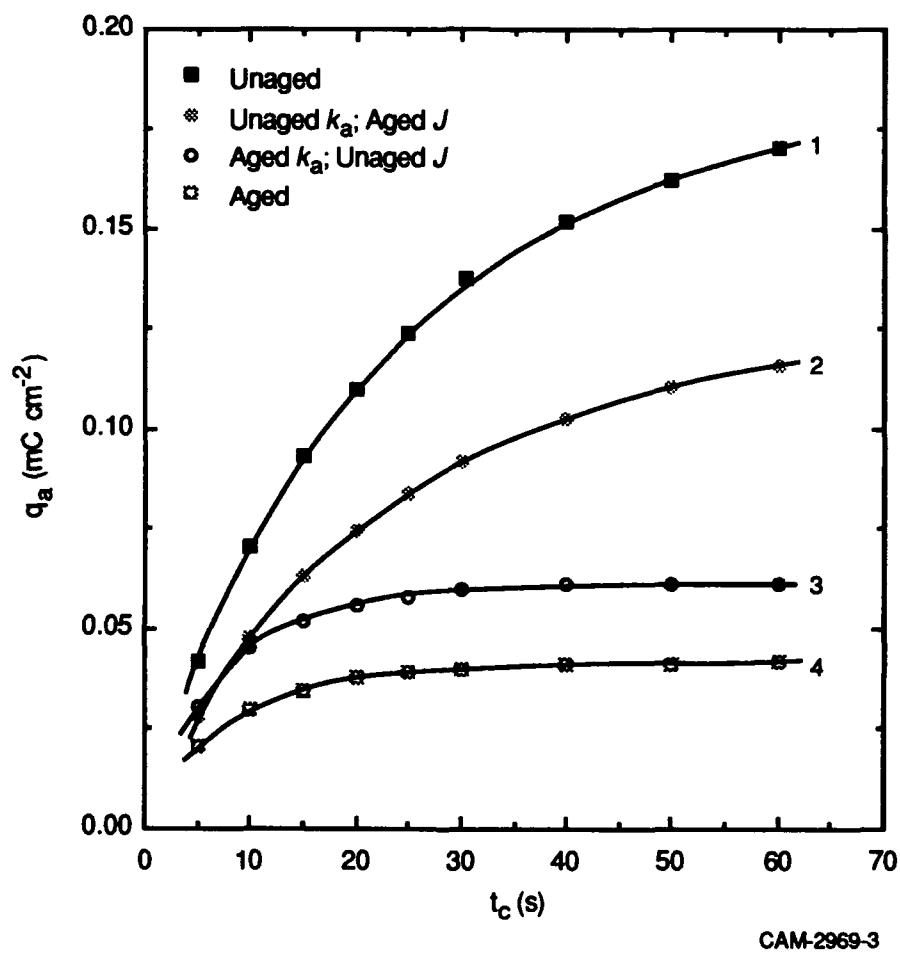
13

CAM-2969-3

Figure 3. Dependence of q_a on charging time for Beta-C Ti.
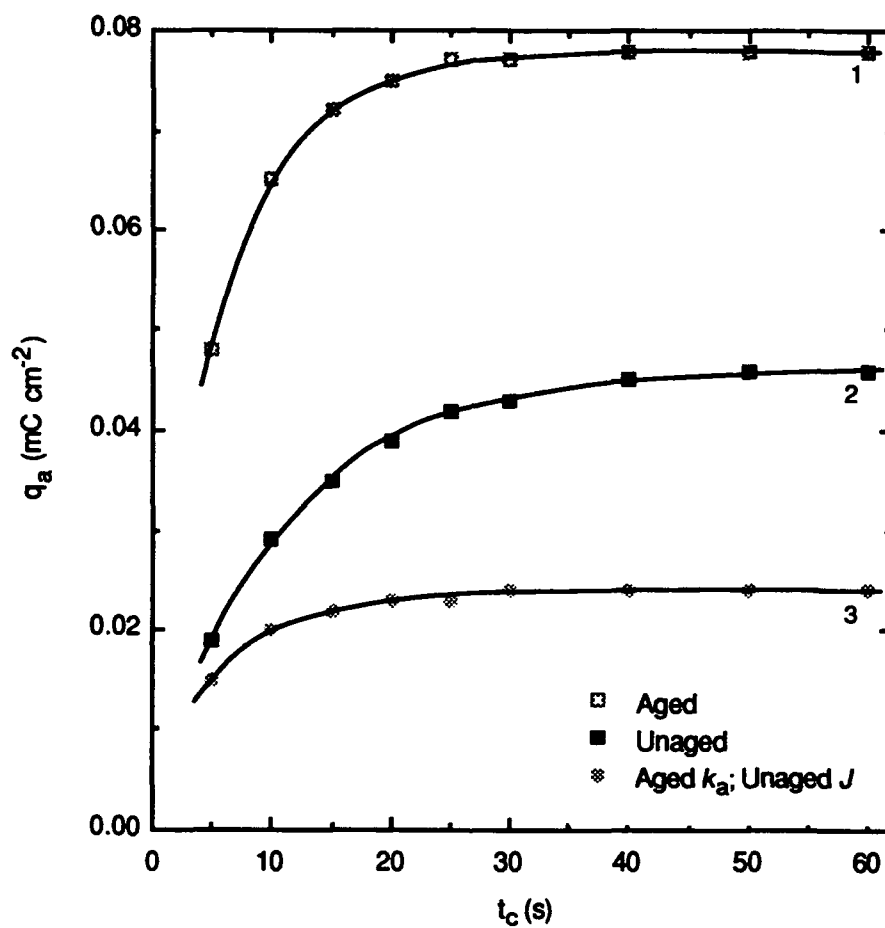$\eta = -0.45$ V.

14

Nevertheless, the change in q_a was still modest, with the result that the trapping constants were subject to some scatter.

Values of k_a and J for two tests on both the unaged and aged alloy are shown in Table 5. In both cases, k_a appeared to be independent of charging potential, despite considerable scatter in some tests for the unaged alloy and the uncertainty in fitting the experimental data for the aged alloy. The overall mean values of k_a for the unaged and aged alloys were 0.069 ± 0.011 s^{-1} and 0.15 ± 0.01 s^{-1}, respectively. Again, the flux showed the expected increase with potential in both cases. However, the flux for Ti-13-11-3, unlike that for Beta-C Ti, increased with aging, presumably because of the considerably more negative charging potentials used for the aged alloy.

The variation in q_a calculated using the values of k_a and J at $\eta = -0.55$ V is shown in Fig. 4. The top and middle curves (1 and 2) represent data for the aged and unaged alloys, respectively, whereas curve 3 corresponds to the aged condition but with J limited to that for an unaged surface. The increase in k_a without a change in J (curve 3), as noted above, acts to decrease not only q_a but also its dependence on t_c. The principal effect of a higher J on curve 3 is to raise q_a, resulting in curve 1 for the aged alloy.

Table 5
VALUES OF k_a AND J FOR TI-13V-11Cr-3Al

State	Test	η (V)	E$_c$ (V/SCE)	k_a (s^{-1})	J (nmol cm^{-2} s^{-1})	Mean k_a
Unaged	11	-0.45	-0.479	0.072	0.048	
		-0.50	-0.523	0.064	0.051	0.069 ± 0.004
		-0.55	-0.574	0.072	0.067	
	12	-0.40	-0.428	0.066	0.033	
		-0.45	-0.473	0.043	0.046	0.068 ± 0.018
		-0.50	-0.524	0.094	0.086	
Aged	13	-0.45	-0.984	0.15	0.13	
		-0.50	-1.038	0.14	0.17	0.14 ± 0.01
		-0.55	-1.094	0.14	0.22	
	14	-0.50	-1.050	0.15	0.18	
		-0.55	-1.119	0.17	0.26	0.16 ± 0.01

CAM-2969-4

Figure 4. Dependence of q_a on charging time for Ti-13V-11Cr-3Al.
$\eta = -0.55$ V.

16

Ti-6Al-4V

Values of k_a and J for two tests on this as-received alloy are shown in Table 6. As with the β-Ti alloys, k_a is essentially independent of charging potential, and the flux increases with potential. The mean value of k_a for both tests was 0.063 ± 0.005 s^{-1}.

Table 6
VALUES OF k_a AND J FOR TI-6Al-4V

Test	η (V)	E_c (V/SCE)	k_a (s^{-1})	J (nmol cm^{-2} s^{-1})	Mean k_a
15	-0.60	-0.782	0.061	0.070	
	-0.65	-0.846	0.066	0.107	0.064 ± 0.002
16	-0.55	-0.624	0.068	0.078	
	-0.60	-0.674	0.056	0.078	0.062 ± 0.004
	-0.65	-0.731	0.064	0.095	
	-0.70	-0.799	0.060	0.116	

COPPER-NICKEL ALLOYS

Marinel

Values of k_a and J for two tests on Marinel are given in Table 7. In both cases, k_a was independent of charging potential. The overall mean value of k_a was 0.034 ± 0.004 s^{-1}. As with the Ti alloys, the flux generally increased with potential.

Monel K-500

Values of k_a and J for tests on both the unaged and aged alloy are given in Table 8. In both cases, k_a was independent of charging potential. The overall mean values of k_a for the unaged and aged alloys were 0.017 ± 0.003 s^{-1} and 0.021 ± 0.003 s^{-1}, respectively. Again, the flux generally increased with potential.

The trapping constant for the aged alloy is in agreement with the average value (0.021 s^{-1}) obtained for a range of electrolytes in our earlier work. Although in the earlier

work on Monel K-500 there was no apparent difference in trapping behavior between the unaged and aged alloy, subsequent improvements in the precision of the data now indicate that the trapping constant of the aged alloy may be a little higher than that of the unaged alloy.

Table 7
VALUES OF k_a AND J FOR MARINEL

Test	η (V)	E_c (V/SCE)	k_a (s^{-1})	J (nmol cm^{-2} s^{-1})	Mean k_a
17	-0.25	-0.355	0.027	0.045	
	-0.30	-0.407	0.040	0.049	
	-0.35	-0.460	0.037	0.054	
	-0.40	-0.512	0.036	0.056	0.034 ± 0.004
	-0.55	-0.665	0.032	0.059	
	-0.60	-0.710	0.031	0.070	
18	-0.25	-0.374	0.034	0.038	
	-0.35	-0.471	0.037	0.040	
	-0.40	-0.524	0.029	0.036	
	-0.45	-0.577	0.039	0.043	0.035 ± 0.003
	-0.50	-0.630	0.036	0.045	
	-0.55	-0.678	0.032	0.057	

Table 8
VALUES OF k_a AND J FOR MONEL K-500

State	Test	η (V)	E_c (V/SCE)	k_a (s^{-1})	J (nmol cm^{-2} s^{-1})	Mean k_a
Unaged	19	-0.30	-0.386	0.014	0.095	
		-0.35	-0.442	0.025	0.137	
		-0.40	-0.495	0.021	0.133	
		-0.45	-0.548	0.017	0.128	0.018 ± 0.003
		-0.50	-0.602	0.016	0.143	
		-0.55	-0.660	0.017	0.164	
	20	-0.25	-0.333	0.015	0.058	
		-0.30	-0.384	0.017	0.070	
		-0.35	-0.439	0.014	0.071	0.015 ± 0.001
		-0.40	-0.492	0.013	0.082	
Aged	21	-0.25	-0.344	0.023	0.046	
		-0.30	-0.388	0.015	0.062	
		-0.35	-0.432	0.022	0.107	0.020 ± 0.003
		-0.40	-0.480	0.022	0.137	
		-0.45	-0.528	0.018	0.153	
	22	-0.25	-0.319	0.018	0.083	
		-0.30	-0.372	0.026	0.184	
		-0.35	-0.423	0.024	0.201	0.022 ± 0.003
		-0.45	-0.526	0.022	0.199	
		-0.50	-0.578	0.019	0.202	
	23	-0.25	-0.310	0.018	0.100	
		-0.30	-0.366	0.022	0.146	
		-0.35	-0.417	0.022	0.176	0.020 ± 0.002
		-0.40	-0.468	0.021	0.192	
		-0.45	-0.520	0.017	0.184	

19

DISCUSSION

TITANIUM ALLOYS

Irreversible Trapping Constants

The mean values of the trapping constants for the β-titanium alloys and Ti-6-4 are summarized in Table 9. Also shown are data obtained for titanium grade 2 in some of our previous work using HIAPP.[7] The irreversible trapping constant (k) can be derived from k_a by using diffusivity data for the "pure" alloy to obtain the lattice diffusivity (D_L) and for the actual alloy to obtain the apparent diffusivity (D_a). The "pure" alloy is considered to be Ti with its principal alloying elements, so that minor elements are assumed to be primarily responsible for reversible trapping in the actual alloys.

Table 9
TRAPPING CONSTANTS FOR TITANIUM ALLOYS

Alloy	State	Phase[a]	k_a (s^{-1})	D_L/D_a	k (s^{-1})
Single-Phase					
Ti Grade 2	Unaged (low H)[b]	α	0.028 ± 0.002	1	0.028
Beta-C Ti	Unaged	β	0.031 ± 0.002	≥ 1	≥ 0.031
Ti Grade 2	Unaged (high H)[b]	α	0.040 ± 0.004	1	0.040
Multi-Phase					
Ti-6-4	As-received	α_p-β	0.063 ± 0.005	≥ 1	≥ 0.063
Ti-10-2-3	Aged	β-α_s	0.066 ± 0.009	≥ 1	≥ 0.066
Ti-13-11-3	Unaged	β-α_p	0.069 ± 0.011	≥ 1	≥ 0.069
Beta-C Ti	Aged	β-α_s	0.088 ± 0.010	≥ 1	≥ 0.088
Ti-13-11-3	Aged	β-α_{p+s}	0.15 ± 0.01	≥ 1	≥ 0.150

[a] α_p = primary α phase; α_s = secondary α phase.
[b] When the charging potential reaches approximately -0.93 V, k_a increases from 0.028 to 0.040 s^{-1}.[7]

The role of defects such as vacancies and edge dislocations in reversible trapping should also be considered, but their effect can be treated as secondary on the basis of a comparison of hydrogen transport in other metals. Whereas the lattice diffusivity of hydrogen in iron is high enough to be affected by reversible trapping, the transport of hydrogen in fcc metals appears to be limited by diffusion itself, with little hindrance from defects such as vacancies or edge dislocations.[11] The diffusivity for β-titanium at 25°C is intermediate between those for iron and nickel; for example, the diffusivity for Ti-13-11-3 is 2.7×10^{-11} m^2 s^{-1} at 25°C.[12] Hence, as in most studies of palladium ($D_L = 1$-4.5×10^{-11} m^2 s^{-1}),[13-15] the diffusivity is assumed to be low enough that reversible trapping at defects can be ignored.

In the case of Ti grade 2, the irreversible trapping constant for Ti alloys can be approximated to the apparent trapping constant on the basis of the low diffusivity of hydrogen in α-Ti (1.65×10^{-16} m^2 s^{-1} at 25°C)[16] and the closeness in the composition of the grade 2 metal and pure titanium. Because of these factors, the diffusivities for the pure and commercial grades are assumed to differ negligibly, so that $D_a \approx D_L$ and therefore $k \approx k_a$.

The situation regarding D_a is more debatable for the β-titanium alloys. Few data are available in the literature for the diffusivity of hydrogen in these alloys, with or without minor alloying elements. As a rough approximation, the minor elements in the β-Ti alloys also can be assumed to contribute only slightly to reversible trapping for diffusivities on the order of 10^{-11} m^2 s^{-1}. In effect, this assumption allows a lower limit to be determined for k in each case (Table 9), since trapping invariably causes $D_a < D_L$ and therefore $k > k_a$.

Effect of Aging

Commercial β-Ti alloys such as Ti-10-2-3 and Beta-C contain as much as 60% α phase in their optimally heat-treated conditions. The presence of the α phase increases the possibility of hydride formation either in the α phase or at the α/β interface.[17] In α-β Ti alloys, hydrogen segregates to the interface between the two phases and forms brittle hydrides at these sites, with growth occurring preferentially into the α phase.[18] The tendency to hydride formation is expected to decrease as the volume fraction of β phase increases, and therefore β alloys should be less prone to hydride induced embrittlement than near-α or α-β alloys.

Various studies do indeed indicate that hydrogen embrittlement of fully β-phase Ti alloys is not associated with hydride precipitation. For example, Ti-20V suffers a loss of ductility when exposed to hydrogen, but no hydrides are apparent except possibly at very high levels.[1] Likewise, annealed, fully β-phase Ti-13-11-3 can be embrittled without forming detectable hydride platelets.[2] Accordingly, a pronounced difference in the trapping characteristics of unaged and aged β-Ti alloys should be observable.

Irreversible trapping constants were evaluated for both the unaged and aged β-titanium alloys studied in this work. Although the values shown in Table 9 represent lower limits, the results indicate clearly that k increases markedly with aging. The additional trapping is undoubtedly associated with the precipitation of secondary α phase, as discussed in detail elsewhere.[19] Even Ti-13-11-3, which contained primary α phase, showed a large increase in k after aging. Interestingly, the trapping constants for unaged Ti-13-11-3 and the α-β alloy, Ti-6-4, are comparable with that for aged Ti-10-2-3 but a little smaller than that for aged Beta-C Ti, indicating that an equivalent level of trapping can be achieved by either primary or secondary α, and that k is sensitive to the amount of secondary α.

Coupled with the evidence[18] concerning hydride sites, the higher k for the aged alloys suggests that irreversible trapping occurs at the α/β interface, presumably in addition to occurring at other sites that are present also in the unaged alloys. Irreversible trapping at the α/β interface, and possibly in the α phase (primary or secondary) if hydrides grow in from the interface, implies that any diffusion of hydrogen through nonhydrided α phase should be negligible. The α phase should therefore have little influence on diffusivity in terms of reversible trapping, and so D_a is considered to have the same value for the aged and unaged alloys.

The trapping character of unaged and aged Beta-C Ti is consistent with somewhat equivocal results of sustained load tests on cathodically charged notched tensile specimens.[20] The load tests showed that solution-treated but unaged Beta-C Ti did not crack during exposure for 720 h (30 days), whereas solution-treated and aged alloy cracked after 175 h. However, the cracking behavior was compared in terms of percent of yield strength, so the applied stress was different for the two conditions, making it uncertain whether stress level or microstructure was the controlling factor. The aged alloy may not have cracked at the stress level of the unaged specimen. Nevertheless, if hydrides were

involved, the aged Beta-C Ti with its α phase should be more susceptible to hydrogen embrittlement than the unaged alloy,[20] as indicated by the trapping constants.

Aging was also found to affect the passive film and therefore the hydrogen entry flux. For example, J showed a considerable decrease for the Beta-C alloy, and so aging in this case produces two opposing effects in terms of hydrogen embrittlement: a reduction in hydrogen entry rate and an enhanced trapping capability.

Identification of Traps in Unaged Alloys

In the absence of α phase, the trapping constants must be interpreted in terms of some other microstructural feature(s). In Ti grade 2, interstitial nitrogen is thought to be the principal irreversible trap at low hydrogen levels.[7] However, a different type of trap seems to predominate in the β-Ti alloys. Ti grade 2 contains 0.007 N compared with 0.018 N in Beta-C Ti, for example, yet the trapping constants have similar values (0.028 and 0.031 s^{-1}, respectively). The implication is either that the trapping character of nitrogen differs between the two phases or that the β phase alloy provides a more dominant irreversible trap.

In view of the wide range of elements in the β alloys, a difference in the type of trap is considered to be the likely reason for the apparent disparity between nitrogen content and trapping capability. Other workers[21] have found that Ti-10-2-3 contains Ti(PSSi) particles, and our previous studies[3-6] using HIAPP have shown that nonmetallic inclusions and precipitates are generally the predominant irreversible traps in various alloys. Accordingly, the irreversible traps in Ti-10-2-3, and possibly the other β-Ti alloys,[21] are believed to be Ti(PSSi) particles. As noted above, this hypothesis can be tested by comparing the density of trap particles calculated from k_a [Eq. (3)] with the actual concentration of particles. Calculation of the trap density involves the particle radius, which, in conjunction with the particle concentration, will be determined from microstructural studies to be performed on the unaged alloys during the rest of this work.

COPPER-NICKEL ALLOYS

Irreversible Trapping Constants

The mean values of the trapping constants for the two nickel-containing alloys are given in Table 10. Evaluation of k from k_a requires diffusivity data for the pure Ni-Cu

alloy to obtain D_L and for Monel K-500 or Marinel to obtain D_a. As in our previous work[3-6] on nickel-base alloys, the minor alloying elements are assumed to be primarily responsible for the reversible trapping behavior in the Monel because the binding energy of hydrogen to defects in an fcc lattice is a factor of 4 smaller than the activation energy for diffusion.[11]

Table 10
TRAPPING CONSTANTS FOR COPPER-NICKEL ALLOYS

Alloy	State	k_a (s^{-1})	D_L/D_a	k (s^{-1})
Marinel	Aged	0.034 ± 0.004	1-2	0.034-0.068
Monel K-500	Unaged	0.017 ± 0.003	2.0	0.034
Monel K-500	Aged	0.021 ± 0.003	2.0	0.042

Monel K-500. The diffusivity of hydrogen is 3×10^{-14} m^2 s^{-1} in 30 at% Cu-70 at% Ni at 25°C[22] and 1.48×10^{-14} m^2 s^{-1} in cold-worked and aged Monel K-500 (assumed to be at ambient temperature).[23] The levels of Cu and Ni differ slightly in the 30 Cu-70 Ni alloy and the Monel, but the error in using the diffusivity of the 30 Cu-70 Ni alloy for D_L is considered to be negligible. Accordingly, by using these data for D_L and D_a, the value of k for the aged Monel is found to be 0.042 ± 0.006 s^{-1}.

No data were available for the diffusivity in unaged Monel K-500. Hence, since D_a for the aged Monel is only about a factor of 2 smaller than D_L, it is assumed that the intermetallic particles precipitated during aging have little effect on D_a compared with that of the minor alloying elements in solid solution. On this basis, the value of k for the unaged Monel is 0.034 ± 0.006 s^{-1}.

Marinel. The diffusivity of hydrogen in Marinel has apparently not been reported, so D_a must be estimated from other data. In contrast, D_L can be assigned a value of 1.6×10^{-15} m^2 s^{-1} by using the diffusivity for 77 wt/% Cu-23% Ni.[22] Although the Ni content is lower in Marinel (15% Ni), any effect on D_L can be ignored because of the uncertainty associated with estimating D_a.

Estimating D_a for the Marinel with any reliability is doubtful and so it is more useful to identify limiting values. The upper limit of D_a is essentially determined by D_L, while the lower limit can be evaluated by considering the data for Monel K-500. The value of D_L for the Marinel-base (77 Cu-23 Ni) alloy is an order of magnitude smaller than that for the Monel-base (30 Cu-70 Ni) alloy, so traps could be expected to have less effect in Marinel; that is, the difference between the activation energy for diffusion and the binding energy for reversible traps is likely to be even larger than that for Monel. Hence, we would expect $D_L/D_a < 2.0$ for Marinel, and so $0.034 < k < 0.068$.

Comparison of Ingress Characteristics

The apparent trapping constant for Marinel (aged) is higher than that for Monel K-500 (unaged and aged), but the more meaningful parameter in terms of hydrogen embrittlement is k. The uncertainty in the value of k for Marinel precludes an accurate comparison, but it is possible that the Marinel has an irreversible trapping capability comparable to that of aged Monel; that is, $k \approx 0.042$ s^{-1} for Marinel. This situation would require that $D_L/D_a \approx 1.23$ for Marinel, and therefore that $D_a \approx 1.3 \times 10^{-14}$ m^2 s^{-1}. This value is plausible with respect to D_L for Marinel, which raises the possibility that the irreversible trapping constants for the two aged alloys could well be close enough not to be a deciding factor in distinguishing between their susceptibilities to hydrogen embrittlement. However, this situation does not apply to unaged Monel ($k = 0.034$ s^{-1}), since D_L/D_a would have to be ~1 for Marinel to achieve a similar value of k. Hence, a difference in susceptibility would be expected on the basis of the irreversible trapping constants, with unaged Monel predicted to be less susceptible than either Marinel or aged Monel.

A more obvious difference between the two aged alloys is that Marinel has a smaller entry flux, typically by a factor of 2-3. The implication is that, if the two alloys have a similar trapping capability, Marinel should be less susceptible to hydrogen embrittlement on the basis that hydrogen will build up more slowly to the critical level required to initiate cracking. Slow strain rate tests[24] have been performed on Marinel and Monel K-500 precharged and subsequently maintained at -1.0 V (SCE) in 3.5% NaCl. Both alloys appear to have been tested in the aged condition. The Monel was found to undergo a marked decrease in elongation and reduction of area, whereas Marinel of similar strength exhibited little change after exposure for approximately twice as long. Since the trapping constants for the two aged alloys are probably not significantly different, the smaller flux

appears to account, at least partly, for the lower susceptibility to hydrogen embrittlement reported for Marinel.

SUMMARY

The ingress of hydrogen in three β-titanium alloys (Beta-C, Ti-10V-2Fe-3Al, and Ti-13V-11Cr-3Al), an α-β titanium alloy (Ti-6Al-4V), and two copper-nickel alloys (Marinel and Monel K-500) can be analyzed using a diffusion/trapping model under interface control conditions. The principal findings are summarized as follows:

- Only a lower limit could be determined for the irreversible trapping constant (k) in each case, but the results indicated clearly that k increases markedly with aging. The higher k for the aged alloys appears to be associated with irreversible trapping at the α/β interface, presumably in addition to that occurring at other sites that are present also in the unaged alloys.

- The trapping constants for unaged and aged conditions of Beta-C Ti are consistent with their relative susceptibilities to hydrogen embrittlement as indicated (albeit with some question) by the results of sustained load tests.

- Aging also affects the passive film and therefore the hydrogen entry flux. In the case of Beta-C Ti, aging produces two opposing effects in terms of hydrogen embrittlement — a reduction in hydrogen entry rate and an enhanced trapping capability.

- The principal irreversible trap in unaged Beta-C Ti does not appear to be interstitial nitrogen, as is thought to be case for Ti grade 2 at low hydrogen levels. Instead, Ti(PSSi) particles are believed to provide the principal type of trap in unaged Beta-C Ti.

- The apparent trapping constant for Marinel (aged) is higher than that for Monel K-500 (unaged and aged), but estimates indicate that the irreversible trapping constants for the two aged alloys are likely to be close enough not to be a deciding factor in distinguishing between their susceptibilities to hydrogen embrittlement. However, unaged Monel and Marinel would be expected to differ in susceptibility on the basis of the irreversible trapping constants, with unaged Monel predicted to be less susceptible than either Marinel or aged Monel.

27

- A more obvious difference between the aged Monel and Marinel is that Marinel has a smaller entry flux, so hydrogen will build up more slowly to the critical level required to initiate cracking. Since the trapping constants for the two aged alloys are probably not significantly different, the smaller flux appears to account, at least partly, for the lower susceptibility to hydrogen embrittlement reported for Marinel.

REFERENCES

1. N. E. Paton, R. A. Spurling, and C. G. Rhodes, in *Hydrogen Effects in Metals: Proceedings of the Third International Conference on the Effect of Hydrogen on Behavior of Materials*, I. M. Bernstein and A. W. Thompson, Eds., Moran, Wyoming, 1980 (The Metallurgical Society of AIME, Warrendale, Pennsylvania, 1981), p. 269.

2 B. G. Pound, *Corrosion* 45, 18 (1989).

3. B. G. Pound, *Corrosion* 46, 50 (1990).

4. B. G. Pound, *Acta Metall.* 38, 2373 (1990).

5. B. G. Pound, *Acta Metall.* 39, 2099 (1991).

6. B. G. Pound, *Corrosion* 47, 99 (1991).

7. R. McKibbin, D. A. Harrington, B. G. Pound, R. M. Sharp, and G. A. Wright, *Acta Metall.* 35, 253 (1987).

8. B. G. Pound, R. M. Sharp, and G. A. Wright, *Acta Metall.* 35, 263 (1987).

9. D. Warmuth, Astro Metallurgical, personal communication (1992).

10. W. D. Wilson and S. C. Keeton, in *Advanced Techniques for Characterizing Hydrogen in Metals*, N. F. Fiore and B. J. Berkowitz, Eds. (The Metallurgical Society of AIME, Warrendale, Pennsylvania, 1981), p. 3.

11. W. R. Holman, R. W. Crawford, and F. Paredes, Jr., *Trans. Met. Soc. AIME* 233, 1836 (1965).

12. M.A.V. Devanathan and Z. Stachurski, *Proc. R. Soc. London, Ser. A* 270 (1962) 90.

13. M. Fullenwider, *J. Electrochem. Soc.* 122 (1975) 648.

14. J. G. Early, *Acta Metall.* 26 (1978) 1215.

15. I. I. Phillips, P. Poole, and L. L. Shreir, *Corros. Sci.* 14, 533 (1974).

16. J. E. Costa, D. Banerjee, and J. C. Williams, in *Beta Titanium Alloys in the 1980's*, R. R. Boyer and H. W. Rosenberg, Eds. (The Metallurgical Society of AIME, Warrendale, Pennsylvania, 1984), p. 69.

17. J. D. Boyd, *Trans. ASM* 62, 977 (1969).

18. P. A. Blanchard, R. J. Quigg, F. W. Schaller, E. A. Steigerwald, and A. R. Troiano, WADC Technical Report 59-172, Wright-Patterson Air Force Base, Ohio (April, 1959); cited in Ref. 11.

19. T. W. Duerig and J. C. Williams, in *Beta Titanium Alloys in the 1980's*, R. R. Boyer and H. W. Rosenberg, Eds. (The Metallurgical Society of AIME, Warrendale, Pennsylvania, 1984), p. 19.

20. D. E. Thomas and S. R. Seagle, in *Titanium Science and Technology: Proceedings of the Fifth International Conference on Titanium*, Vol. 4, G. Lütjering, U. Zwicker, and W. Bunk, Eds., Munich, Germany, 1984, p. 2533.

21. T. W. Duerig, G. T. Terlinde, and J. C. Williams, *Metall. Trans.* 11A, 1987 (1980).

22. H. Hagi, *Trans. Jpn. Inst. Metals* 27, 233 (1986).

23. J. A. Harris, R. C. Scarberry, and C. D. Stephens, *Corrosion* 28, 57 (1972).

24. R. Butler, paper presented at Conference on Marine Engineering with Copper Nickel, London, England (1988); cited in "Hiduron Marinel Alloy," Technical Data Sheet, Langley Alloys Ltd., Berks, England (1991).